LETTER

Low-Cost Learning-Based Path Loss Estimation Using Correlation Graph CNN

Keita IMAIZUMI[†], *Student Member*, Koichi ICHIGE[†a)], Tatsuya NAGAO[††], *and* Takahiro HAYASHI[††], *Members*

SUMMARY In this paper, we propose a method for predicting radio wave propagation using a correlation graph convolutional neural network (C-Graph CNN). We examine what kind of parameters are suitable to be used as system parameters in C-Graph CNN. Performance of the proposed method is evaluated by the path loss estimation accuracy and the computational cost through simulation.

key words: *path loss estimation, radio propagation, machine learning, convolutional neural network*

1. Introduction

The radio wave propagation environment needs to be accurately predicted when designing and selecting base stations for mobile communication systems to achieve high-speed communication. Empirical and deterministic models are two typical methods used to predict radio wave propagation [1]. The empirical model is obtained by statistically processing and formulating the measurement data, whose examples include the Okumura-Hata model [2] and the Walfisch-Ikegami model [3], [4]. On the other hand, a deterministic model is used to estimate radio propagation characteristics on the basis of electromagnetic field theory, such as the finite-difference time-domain (FDTD) method [5] and ray tracing method [6].

Prediction methods based on machine learning have already been developed as in [7]–[9]. The training dataset in those methods is constructed using simulations with ray tracing or actual measurement data, and a prediction model is built by using supervised learning. Among them, the KDDI's prediction model [9] evaluates measurement data obtained in urban areas. It uses spatial data such as aerial photographs and building map images, and it uses system parameters such as base station specifications and transmission-reception (Tx-Rx) distances as input data.

We previously extended KDDI's method to estimate building maps from aerial photographs [10]–[13]. Those methods use spatial data around the Tx-Rx midpoint in addition to the Tx and Rx, and the aforementioned machine learning models use a convolutional neural network (CNN) and a fully-connected neural network (FNN). The problem in the machine learning methods is that, when using spatial data, the calculation time and the number of the system parameters increase when using spatial images as the inputs in the learning stage.

Recall that the correlation graph (C-Graph) CNN [14] is a computationally efficient version of CNN, i.e., it does not use spatial image data as the input in the learning stage. Introducing C-Graph CNN to the path loss estimation problem may work well while reducing computational cost. However, so far we have no idea which parameters are suitable to be used as system parameters.

In this paper, we apply the C-Graph CNN to the path loss estimation problem, as a low-cost version without spatial data in the learning stage. We see which feature parameter extracted from spatial data is more appropriate for the path loss estimation. Performance of the proposed method is evaluated in comparison with the FNN-only version of our previous work [11]–[13], using Kokura and Tsudanuma datasets in the propagation database provided by IEICE Technical Committee of Antennas and Propagation [15].

2. Correlation Graph CNN [14]

The C-Graph CNN has been proposed as a computationally efficient version of CNN without using spatial data [14]. The overview of C-Graph CNN is illustrated in Fig. 1. Assume we have a dataset with n feature parameters and m samples for each parameter. We first arrange given data into an $m \times n$ matrix form where the m-th row n-th column ele-

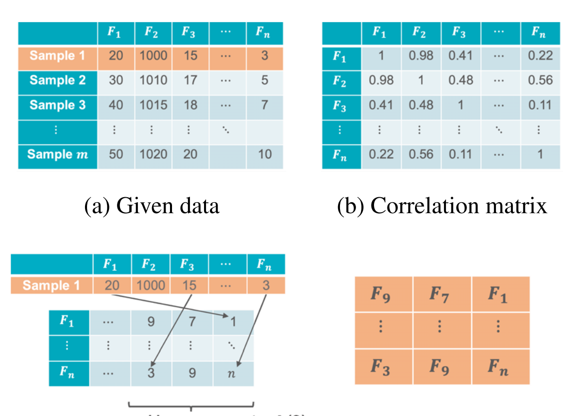

(a) Given data (b) Correlation matrix

(c) Index matrix (d) Data matrix used in CNN

Fig. 1 Overview of C-Graph CNN.

Manuscript received November 17, 2022.
Manuscript revised December 26, 2022.
Manuscript publicized January 26, 2023.

[†]The authors are with Department of Electrical and Computer Engineering, Yokohama National University, Yokohama-shi 240-8501 Japan.
[††]The authors are with KDDI Research Inc., Fujimino-shi 356-8502, Japan.
a) E-mail: koichi@ynu.ac.jp

DOI: 10.1587/transfun.2022EAL2094

ment corresponds to the m-th sample value of the n-th feature parameter as in Fig. 1(a). Then we calculate the correlation coefficients between the features and create an $n \times n$ correlation matrix as in Fig. 1(b). After that, we create the index matrix by sorting and indexing the correlation matrix elements as in Fig. 1(c), see [14] for details. Here we extract only k right (high correlation) columns and remove the remaining left (low correlation) columns so that we have an $n \times k$ index matrix. Finally, by substituting the feature values corresponding to the indices in the $n \times k$ index matrix, we obtain an $n \times k$ matrix as in Fig. 1(d) that enables a convolution operation by CNN.

3. Proposed Method

3.1 Path Loss Estimation Using C-Graph CNN

We construct an estimation model on the basis of C-Graph CNN as in Fig. 2, which consists of one convolutional layer and two fully-connected layers. Here we use nine system parameters: four fundamental radio propagation parameters listed in the first four lines in Table 1, which are often used in path loss estimation problems [11], and five newly introduced parameters that are considered to be suitable for the proposed model and whose details are described in Sects. 3.2 and 3.3. Note that there is only one base station in each of Kokura and Tsudanuma dataset [15], therefore the parameters related to Tx are ineffective and removed in this paper.

The training time is expected to be significantly reduced compared with a conventional CNN-based model like [11], because the model does not use images as the input. Note that the input correlation matrix can be regarded as two-dimensional data like images, but the matrix is much smaller than the input map images. Moreover, this model is expected to improve the estimation accuracy compared with the FNN-based model, because the column order of the input matrix was modified so that it clearly represents the features of the input parameters.

3.2 Extended Building Occupancy Rate

We use the building occupancy rate as an indicator of the radio propagation environment to estimate propagation loss. This is based on a building map image that expresses the presence or absence of buildings as a binary value and shows the rate of buildings on a straight line connecting the Tx and Rx points. Note that the building occupancy rate itself has often been used in our previous papers [11]–[13] as a ratio of the building existence on a Tx-Rx line. We extend the definition of the rate on not only the Tx-Rx line but also the multiple neighboring lines drawn as the colored lines in Fig. 3(a), so as to consider not only direct waves but also the effects of diffracted and/or reflected waves. Note that the building occupancy #1 to #4 in Table 1 respectively correspond to the red, yellow, green and blue lines in Fig. 3(a). Those lines could be combined and/or widened, but as far as our pre-simulations, they works effectively if we deal the four colored lines separately.

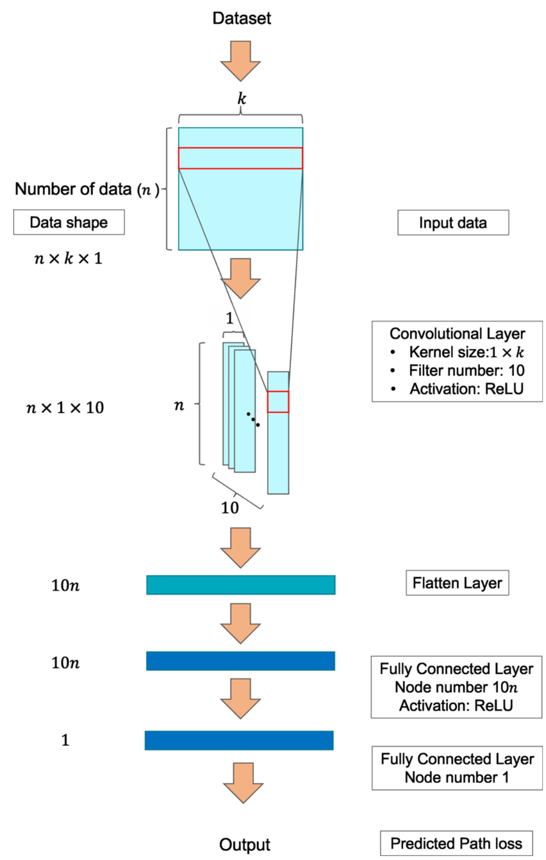

Fig. 2 Proposed model for path loss estimation.

Table 1 System parameters and their correlation against path loss components.

Parameter name	Kokura	Tsudanuma
Horizontal angle [deg]	0.46	−0.10
Vertical angle [deg]	−0.76	0.63
2D distance [m]	0.86	0.53
3D distance [m]	0.86	0.53
Building occupancy #1	0.32	0.27
Building occupancy #2	0.34	0.11
Building occupancy #3	0.34	0.24
Building occupancy #4	0.33	0.24
LOS parameter [m]	0.31	0.36

In addition, we also extend the building occupancy rate in the regions around Tx and Rx as in Fig. 3(b), because those regions are also considered to be important for path loss estimation as well as the lines in Fig. 3(a). We will evaluate what kind of combinations of those lines and regions are more suitable through simulation in the next section.

3.3 The Line-of-Sight Parameter

The line-of-sight (LOS) parameter is a measure of the presence or absence of sight between Tx and Rx points. The received power becomes large when there are no interference buildings but becomes lower when there are building(s)

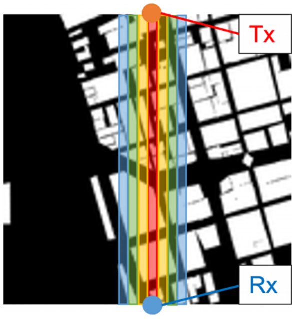

(a) Lines between Tx and Rx

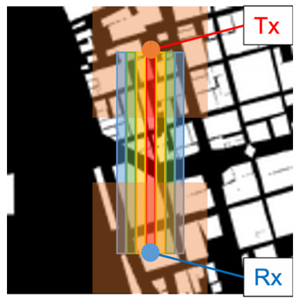

(b) Regions around Tx and Rx

Fig. 3 Regions where the building occupancy rates are calculated.

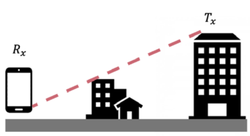

(a) Case of LOS

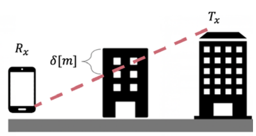

(b) Case of non-LOS

Fig. 4 Difference between LOS and non-LOS.

on the three-dimensional Tx-Rx line as in Fig. 4. Besides, higher buildings will make greater impacts on radio propagation.

On the basis of the above discussion, we define the LOS parameter as a system parameter that considers the effect of interference buildings by

$$\mathrm{LOS} = \begin{cases} 1, & \delta \geq \tau \ \ \text{(non-LOS)} \\ \delta/\tau, & 0 < \delta < \tau \ \ \text{(moderate)} \\ 0, & \delta \leq 0 \ \ \text{(LOS, as in Fig. 4(a))} \end{cases} \tag{1}$$

where δ is the exceeded height as in Fig. 4(b), and τ denotes a threshold height. We add the above-mentioned LOS parameter as one of the system parameters in path loss estimation.

4. Simulation

We evaluate the performance of the proposed path loss estimation method through simulation. The parameters used in the learning stage are shown in Table 2.

In this paper, we evaluate the models using Kokura and Tsudanuma datasets [15] by the root mean square error (RMSE) between the measured and estimated path loss values and compare the performance with that of the two-layer FNN-only model [13], which uses only system parameters without spatial data. We also show the results by the FNN+CNN model [13] for reference, which uses both system parameters and spatial data. The number of data in each dataset is shown in Table 3.

4.1 Estimation Accuracy

Table 4 shows the comparison results of the path loss estimation accuracy in RMSE. We compared the proposed method

Table 2 Parameters for learning.

Activation function	ReLU
Loss function	MSE
Maximum number of epochs	1000
Batch size	32
Optimizer function	Adam
Learning rate	0.001

Table 3 Number of data points in each dataset.

Dataset	Kokura	Tsudanuma
Train	713	825
Test	126	167
Total	839	992

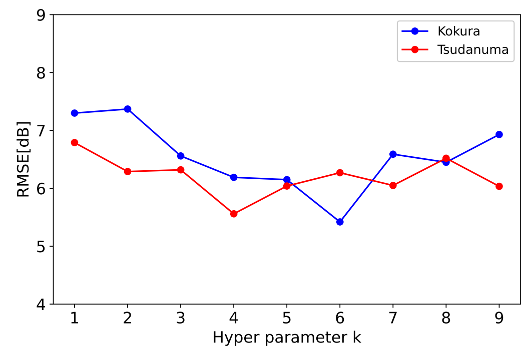

Fig. 5 Behavior of the prediction accuracy in RMSE [dB] as a function of the hyperparameter k.

with the FNN-only model modified from [11] that does not use image data as the input and also with the FNN+CNN model [11] for reference, which uses image data. The threshold τ for the LOS parameter was set to 20 m, which were empirically determined through our pre-simulations.

Note that the number of the columns k extracted from the index matrix was set to 6 for Kokura dataset and 4 for Tsudanuma dataset.

We evaluated the RMSE for various values of the hyperparameter k as shown in Fig. 5, because the number of the index matrix columns k can also be regarded as one of the hyperparameters. We see from Fig. 5 that the RMSE was minimized when $k = 6$ and 4 in Kokura and Tsudanuma datasets, respectively. This is because, the columns with low correlation are not removed and have negative effects when k is a large value. On the other hand, when k is a small value, the columns with high correlation are removed and too much of the data matrix is eliminated, which has a negative effect again. Overall, from the above discussion, the hyperparameter k needs to be defined appropriately in this method. So far from our simulation results, we believe that the optimum value of the hyperparameter k is about half of the number of the inputs.

Table 4 shows that the proposed method improved the RMSE performance against the FNN-only model, and the results in the Tsudanuma dataset were very much improved and close to the results by the FNN+CNN model. This may be because the building occupancy rates at the differ-

Table 4 Comparison of the path loss estimation result in RMSE in [dB].

Model \ Dataset	Kokura	Tsudanuma
FNN only [13]	6.99	8.92
Ours	5.43 ($k = 6$)	5.56 ($k = 4$)
FNN+CNN [13] (reference)	3.53	5.26

Table 5 Prediction accuracy in RMSE [dB].

	Lines only	Lines + Tx region	Lines + Rx region	Lines + Tx/Rx regions
RMSE	5.43	5.56	5.11	5.42

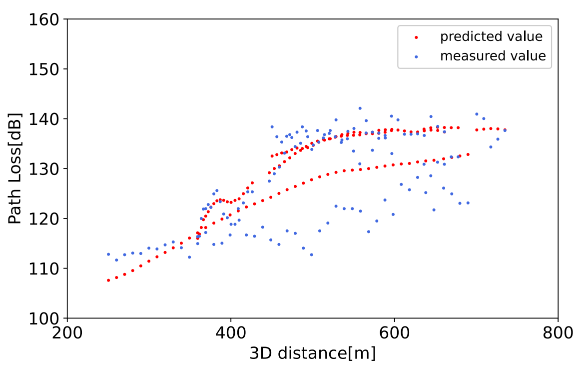

Fig. 6 Path loss distribution as a function of 3-D distance.

ent colored lines in Fig. 3(a) worked well, as indeed Tsudanuma contains many high-rise buildings while Kokura mainly contains low-rise buildings.

4.2 Effect of The Additional Building Occupancy Rate

To evaluate the effectiveness of the additional building occupancy rate proposed at the end of Sect. 3.2, we added an extra system parameter as in Table 5 and evaluated the prediction accuracy. As we see from Table 5, the proposed method achieved the highest accuracy when adding the occupancy rate around the Rx region to the input. This suggests that the occupancy around the receiving point is highly effective in the path loss estimation.

On the other hand, the estimation accuracy was not improved when adding the occupancy rate around Tx region. This is because, the Tx antennas are often installed at the top of high-rise buildings, so it may not be highly correlated with the path loss.

On the basis of the above discussion, we adopted the building occupancy rate on the extended Tx-Rx lines #1-#4 plus around Rx region. We show the 3-D distance characteristics of the path loss estimation results in Fig. 6 when applied to the Kokura dataset. Fig. 6 shows that the estimated points well approximate the original measured points, especially in the upper part of the dataset. The lower part of the data was not well approximated, similar to in [11]. This performance should be improved in future studies.

4.3 Computational Cost

We compared the computational cost and the number of parameters to be trained. The actual training time was about 1.1 seconds per 100 epochs in the proposed model, while it was about 60 seconds in the FNN+CNN method [11]. Besides, the convolutional layer in the proposed method requires only 50 parameters to be trained, while the convolutional layer of the FNN+CNN model [11] requires 19,930 parameters. Compared with the conventional model [11], which uses image data as the input in the learning stage, we found that the computational complexity was significantly reduced.

5. Conclusion

In this paper, we proposed a path loss estimation model using correlation graph convolutional neural network (C-Graph CNN). We examined the system parameters to be used in the learning stage, and the extended building occupancy rate and the line-of-sight (LOS) parameters worked well. Also we found that the proposed method requires only a small computational cost. Future work includes improving the model structure.

Acknowledgments

We thank IEICE technical committee on Antennas and Propagation for the measurement dataset [15].

References

[1] T.K. Sarkar, Z. Ji, K. Kim, A. Medouri and M. Salazar-Palma, "A survey of various propagation models for mobile communication," IEEE Antennas Propag. Mag., vol.45, no.3, pp.51–82, June 2003.
[2] M. Hata, "Empirical formula for propagation loss in land mobile radio services," IEEE Trans. Veh. Technol., vol.29, no.3, pp.317–325, Aug. 1980.
[3] F. Ikegami, S. Yoshida, T. Takeuchi, and M. Umehira, "Propagation factors controlling mean field strength on urban streets," IEEE Trans. Antennas Propag., vol.32, no.8, pp.822–829, Aug. 1984.
[4] J. Walfisch and H.L. Bertoni, "A theoretical model of UHF propagation in urban environments," IEEE Trans. Antennas Propag., vol.36, no.12, pp.1788–1796, Dec. 1988.
[5] Y. Wang, S. Safavi-Naeini, and S.K. Chaudhuri, "A hybrid technique based on combining ray tracing and FDTD methods for site-specific modeling of indoor radio wave propagation," IEEE Trans. Antennas Propag., vol.48, no.5, pp.743–754, May 2000.
[6] S.C. Kim, B.J. Guarino, T.M. Willis, V. Erceg, S.J. Fortune, R.A. Valenzuela, L.W. Thomas, J. Ling, and J.D. Moore, "Radio propagation measurements and prediction using three-dimensional ray tracing in urban environments at 908 MHz and 1.9 GHz," IEEE Trans. Veh. Technol., vol.48, no.3, pp.931–946, May 1999.
[7] E. Ostlin, H. Zepernick, and H. Suzuki, "Macrocell path-loss prediction using artificial neural networks," IEEE Trans. Veh. Technol., vol.59, no.6, pp.2735–2747, July 2010.
[8] T. Imai, K. Kitao, and M. Inomata, "Radio propagation prediction model using convolutional neural networks by deep learning," Proc. 13th European Conference on Antennas and Propagation (EuCAP), pp.1–5, 2019.

[9] T. Hayashi, T. Nagao, and S. Ito, "A study on the variety and size of input data for radio propagation prediction using a deep neural network," Proc. 14th European Conference on Antennas and Propagation (EuCAP), pp.1–5, 2020.
[10] K. Inoue, K. Ichige, T. Nagao, and T. Hayashi, "Radio propagation prediction using deep neural network and building occupancy estimation," IEICE Commun. Express, vol.9, no.10, pp.506–511, Oct. 2020.
[11] K. Inoue, K. Ichige, T. Nagao, and T. Hayashi, "Learning-based prediction method for radio wave propagation using images of building maps," IEEE Antennas Wireless Propag. Lett., vol.21, no.1, pp.124–128, Jan. 2022.
[12] K. Inoue, K. Imaizumi, K. Ichige, T. Nagao and T. Hayashi, "Learning-based path loss estimation using multiple spatial data and system parameters," Proc. IEEE Vehicular Technology Conference (VTC 2022-Fall), no.1G-3, Sept. 2022.
[13] K. Inoue, K. Imaizumi, K. Ichige, T. Nagao, and T. Hayashi, "Path loss estimation using spatial data and neural networks," IEICE Trans. Commun. (Japanese edition), vol.J105-B, no.11, pp.872–879, Nov. 2022.
[14] Y. Hechtlinger, P. Chakravarti, and J. Qin, "A generalization of convolutional neural networks to graph-structured data," arXiv preprint, arXiv:1704.08165, April 2017.
[15] Propagation Database, IEICE Technical Committee on Antennas and Propagation. https://www.ieice.org/cs/ap/misc/denpandb/prop_db/